



HHS Public Access

Author manuscript

Min Metall Explor. Author manuscript; available in PMC 2023 May 17.

Published in final edited form as:

Min Metall Explor. 2022 July 05; 39(5): 1887–1897. doi:10.1007/s42461-022-00655-4.

Exploration of Limestone Pillar Stability in Multiple-Level Mining Conditions Using Numerical Models

Gamal Rashed¹, Brent Slaker¹, Michael Murphy¹

¹CDC/NIOSH/PMRD, Pittsburgh, USA

Abstract

Pillar stability continues to be a significant concern in multiple-level mining conditions, particularly for deep mines when pillars are not stacked or the thickness of interburden between mining levels is thin. The National Institute for Occupational Safety and Health (NIOSH) is currently conducting research to investigate the stability of pillars in multiple-level limestone mines. In this study, FLAC3D models were created to investigate the effect of interburden thickness, the degree of pillar offset between mining levels, and in situ stress conditions on pillar stability at various depths of cover. The FLAC3D models were validated through in situ monitoring that was conducted at a multiple-level stone mine. The critical interburden thickness required to minimize the interaction between the mining levels on top-level pillar stability was explored, where the top level mine was developed first followed by the bottom level mine.

The model results showed that there is an interaction between numerous factors that control the stability of pillars in multiple-level conditions. A combination of these factors may lead to various degrees of pillar instabilities. The highest degree of local pillar instability occurred when pillar overlap ranges between 10 and 70%. On the contrary, the highest degree of stability occurs when the pillars are stacked, the underlying assumption is that the interburden between mining levels is elastic (never fails). Generally, for depths of cover investigated in this study, the stability of top-level pillars shallower than 100 m (328 ft) or with interburden thicknesses greater than 1.33 times the roof span—16 m (52.4 ft) in this study—does not appear significantly impacted by pillar offset. The results of this study improve understanding of multiple-level interactions and advances the ultimate goal of reducing the risk of pillar instability in underground stone mines.

Keywords

Ground control; Limestone; Pillar stability; Interburden stability; Multiple-level; Pillar offset

[✉] Gamal Rashed, grashed@cdc.gov.

Data from this manuscript have been presented at the 40th SME International Conference on Ground Control in Mining, July 27–28, 2021.

Disclaimer The findings and conclusions in this report are those of the authors and do not necessarily represent the official position of the National Institute for Occupational Safety and Health. Mention of any company or product does not constitute endorsement by NIOSH.

1 Introduction

Pillar stability has always been one of the foremost concerns of ground control in underground mining. In underground stone mining, understanding pillar stability was the focus of recent research by the National Institute for Occupational Safety and Health (NIOSH) and led to the creation of recommendations and a pillar design software (S-Pillar) [2, 3, 14]. These recommendations were based on an empirical study that only included single-level mines. The general applicability of the previous research to multiple-level mines is not fully understood and is the subject of a current NIOSH investigation on stone pillar design in challenging conditions. The S-Pillar software has been applied to multiple-level stone mines in the past. However, it would be unwise to use the single-level recommendations without considering potential multiple-level interactions accompanied by a more complete engineering analysis and numerical modeling evaluation [16] and [15]. Multiple-level interactions can manifest as stress changes within the interburden or pillars, which are undesirable if they lead to the failure of either of these structures. When possible, it may be wise to consider the local effects of stress concentrations transferred through levels in the larger mine design. Newman et al. [17] used the LaModel software program to highlight areas of elevated stress imparted from an overlying level and designed the mine in such a way as to minimize the exposure of haul routes and life-of-quarry headings to the increased ground hazard. Rashed and Slaker [18] investigated the interburden stability in underground stone mines using FLAC3D numerical models and found that there is an interaction between multiple factors that control the stability of the interburden. They demonstrated the impact that even small pillar offsets can have on interburden stability in underground stone mines when the interburden thickness is relatively small.

There is a limited body of research for multiple-level underground limestone research, while there is an abundance of research into room-and-pillar multiple-level mining in coal mining [5, 8, 12]. Limestone mines tend to have larger roof spans, larger pillar height, smaller and stronger pillars, less geologic stratification, pillars are usually benched, and do not retreat mine, making the interactions between levels distinctly different than what has been studied previously in coal mines. When discussing multiple-level pillar stability, parameters such as width-to-height ratio and depth are still crucially important, but the interburden thickness and pillar offset must additionally be considered. Pillar offset, which is the degree to which pillars are not columnized or stacked, can occur inadvertently due to blasting problems, surveying errors, or rib failures, and can occur intentionally by mining above or below workings with a geometry that is impossible or unreasonable to match. Larger interburden thicknesses are likely to reduce the impact of pillar offsetting, and the effect of increasing or decreasing interburden thickness will be explored in this paper. Interburden competency is also important, and typically most influenced by thickness and strength, but it is not the focus of this paper.

Stone pillar stability can be influenced greatly by the occurrence of geological discontinuities [9]. Also, weak bands in a stone pillar can significantly reduce its strength, as these bands induce tension in the stronger rock slabs [4]. Instabilities driven by discontinuities or weak bands are not considered in this study. Only stone pillar instability due to overloading is investigated because the influence of both geological discontinuities

and weak bands are highly variable and site specific. Moreover, the main purpose of this work is to better understand the response of a stone pillar to multiple-level mining conditions so it can be applied to situations where the impact of discontinuities or weak bands are either well understood or insignificant. The actual jointed rock mass in this study was replaced with a homogenous isotropic continuum model of equivalent properties. The underlying assumption of the continuum rock mass model used in this study is that rock mass behavior is not dominantly controlled by a single joint set, i.e., all joint sets are equally important. Designing stable mine workings requires a careful consideration of more than just pillar stability, but the authors believe that by making some widely applicable assumptions, there are some general trends that can be observed in pillar performance subjected to multiple-level interactions. In this paper, the authors assume a stable interburden, a stable roof span, and pillars which would be expected to remain stable in a single-level mine layout. The intent of this study is to provide some insight into how stone pillars can be affected by undermining and considerations for ensuring stable pillar design.

2 Study Parameters

In this study, FLAC3D numerical models were created to understand the impact of numerous parameters on pillar stability in two-level underground stone mines. The modeled pillars were assumed in a flat-lying deposit. The modeled pillars are equal-sized pillars of a square cross-sectional area of 12 m (39.4 ft) × 12 m (39.4 ft), a height of 8 m (26.2 ft), and a width-to-height ratio of 1.5. The headings and the crosscuts are 12 m (39.4 ft). The in situ stress field was varied to account for both low and high in situ stress fields encountered in the USA, where the horizontal/vertical stress ratio (k -ratio) is 0.3 and 3.0. The depth of cover ranges from 100 m (328 ft) to 400 m (1,312 ft); this range covers most of the underground stone mines in the USA. The interburden thickness ranges from 4.0 m (13.1 ft) to 32.0 m (104.9 ft). The lowest interburden thickness evaluated for this study, 4 m (13.1 ft), is not common in underground stone mines in the USA. However, it has been considered in this study to show the potential detrimental effects of an extremely thin interburden. The percentage of pillar overlap between the mining levels ranges from 100 to 0%. A 100% pillar overlap refers to pillars that are situated on top of one another, i.e., perfectly columnized/stacked as shown in Fig. 1a, while a 0% overlap refers to a situation where a top-level pillar is completely overlying an opening, as shown in Fig. 1b. This definition of overlap percentages applies strictly to situations where pillar width is equal to opening width, and as a result, caution should be used when interpreting this for other designs.

Pillar overlap is given as the area of the top-level pillar that is directly overlying a bottom-level pillar to capture a complete picture of the effect of pillar overlap on pillar stability. The bottom-level pillars were offset either in the x direction only or in both the x and y directions. When pillars are offset in x and y directions, the offset distance is the same for both directions, so an offset of 1 m in the x direction does not result in the same overlap percent as an offset of 1 m in both the x and y directions. Various pillar overlaps were generated by offsetting the lower-level pillars in the x direction only or in the x and y directions with respect to the upper-level pillars.

Table 1 summarizes the parameters used in the FLAC3D models and the values for each parameter. Numerous combinations of the study parameters were generated to determine when the interaction between the mining levels occurs and how significant the impact of these parameters could be on pillar stability.

3 Laboratory Test Results for Limestone Specimen

The relationship between the strength of samples that can be tested in the laboratory and the strength of the rock mass is particularly important in determining design strength values for stability analysis. Mechanical properties for limestone material used in this study are based on tests conducted and recently collected from a multiple-level limestone mine in the Monteagle Limestone. Eight cylindrical limestone specimens were tested under the conventional triaxial loading conditions to obtain the intact strength and the Hoek–Brown m and s parameters. The ASTM D 7012–04 (Methods C and D) and ASTM D 4543–04 specifications were followed for specimen preparation and testing [1]. The minimum confining pressure was 5.0 MPa (725 psi), and the maximum confining pressure was 25.0 MPa (3,625 psi). Table 2 summarizes the test results for the intact properties of the limestone specimens used in this paper. The laboratory test results were used as an input for the Hoek–Brown material model used in the FLAC3D numerical models. The Young's modulus from the laboratory test results was scaled down to obtain the rock mass modulus [7].

It is important to consider variable mechanical properties—strength and deformability—for limestone material, which is not considered in this paper. This is why the model results are illustrative and are used to raise awareness more than they are to be used for a design purpose.

4 FLAC3D Model Setup

Numerical modeling is a useful tool to investigate local pillar instabilities due to pillar offset between mining levels at various interburden thicknesses, depths, and in situ stress conditions. Numerical models were created using FLAC3D Version 7.0 [10]. The study pillar in the FLAC3D models is located in the middle of a 9×9 array of pillars. The Hoek–Brown criterion and the Geological Strength Index (GSI) have been used to estimate the rock mass properties, such that the generalized Hoek–Brown Failure criterion was selected to model the peak strength of pillars/elements. A strain softening material model is incorporated when the limestone material was loaded beyond its peak strength. The Hoek–Brown failure criterion in principal stress format is shown in Eq. 1 [6].

$$\sigma_1 = \sigma_3 + \sigma_{ci} \left[m_b \frac{\sigma_3}{\sigma_{ci}} + s \right]^a \quad (1)$$

where σ_{ci} is the UCS of limestone material, m_b is a reduced value of the material constant m_i given by Eq. 2:

$$m_b = m_i + \exp\left[\frac{GSI - 100}{28 - 14D}\right] \quad (2)$$

The Geological Strength Index (GSI) was selected to implicitly replicate pre-existing rock mass joints in limestone pillars. A peak GSI of 80 was selected to represent a very good rock mass quality and zero disturbance factor was assumed due to blasting in this study. Using the peak GSI and the D, other Hoek–Brown constants (s and a) can be calculated from Eqs. 3 and 4.

$$s = \exp\left[\frac{GSI - 100}{9 - 3D}\right] \quad (3)$$

$$a = 0.5 + \frac{1}{6}\left[e^{-\frac{GSI}{15}} - e^{-\frac{20}{3}}\right] \quad (4)$$

The softening behavior for limestone material with the plastic shear strain was modeled by varying the GSI from a peak value of 80 to a final value of 10. The Hoek–Brown constants (m , s , and a) should change accordingly. The rock mass modulus for the modeled limestone was estimated from Eq. 5 [7], where E_{rm} and E_i are the rock mass modulus and intact rock modulus, respectively.

$$E_{rm} = E_i \left[0.02 + \frac{1 - \frac{D}{2}}{1 + \exp\left[\frac{60 + 15D - GSI}{11}\right]} \right] \quad (5)$$

The bottom of the FLAC3D model is fixed, while the side boundaries are roller supported to allow only vertical movement. The FLAC3D models were solved in five stages: (1) geostatic stage, in which the pre-mining in situ stresses are initialized, (2) development stage for the top-level mine, in which all headings and crosscuts are excavated in the top level, (3) development stage for the bottom-level mine, in which all headings and crosscuts are fully developed (not partially developed), (4) the material model for top and bottom level pillars was switched from elastic to nonlinear to minimize the dynamic effect generated from mining. Hence, the yield pattern of the study pillar can be explored, and (5) a displacement load was applied on the top of the model to fail the study pillar to obtain its ultimate strength.

5 FLAC3D Model Calibration and Validation

The Hoek–Brown material model with the strain-softening behavior explained in the previous section was used to estimate the peak strength of a single pillar of a width-to-height ratio equal to 1.5. The peak strength from the FLAC3D model was compared to the pillar strength calculated from an empirical pillar strength equation proposed by Lunder and Pakalnis [11]. The predicted strength from Lunder and Pakalnis was about 58 MPa, while the predicted strength from the FLAC3D model was about 60 MPa. Additionally,

the FLAC3D material model has been compared to the instrumentation results of a multiple-level stone mine called “Mine A” which is located in Tennessee. The depth of cover for this mine ranges from 10- to 245-m (32.8 to 803.6-ft). This mine extracts the Monteagle Limestone which is commonly oolitic fine to coarse grained and white to light gray in color [19]. The upper level of the mine is a massive limestone that contains two joint sets dipping at N5E and N56W. Jointing in lower level is more prominent compared to the upper level which causes rib stability issues [19].

The pillar size at upper and lower-level mines is about 13.7 by 13.7 m (44.9 by 44.9 ft). The opening width in both levels is about 15.2 m (49.9 ft). The mining height in both levels is about 9.1 m (29.8 ft). The interburden thickens is relatively thin especially when compared to the excavation width, it ranges from 6 to 8 m (19.6 to 26.2 ft). The upper and lower-level pillars are columnized. Planned dimensions may deviate from mined dimensions, and as a result, pillar offsets of 1 to 2 m (~ 3.2 to 6.5 ft) from the upper level to the lower level are common. The layout of the top and bottom-level mines overlain on each other is shown in Fig. 2. The Rhino 6 software [13] was used to generate the mesh for the mine geometry, which was exported to the FLAC3D to conduct a stress analysis. P1 and P2 are two pillars that were instrumented with vibrating wire stress meters (VWSM). The locations of these stress meters are marked with black circles as shown in Fig. 2b. P1 has VWSM1, while P2 has VWSM2. The element size of the instrumented pillar is 0.25 m (~ 0.8 ft). The interburden thickness between the upper and the lower mines used in the model is 8 m (26.2 ft).

The vertical stress distribution was investigated at profiles A-A and B-B for two loading stages: step 2 represents a full development of the top-level mine and step 3 represents a partially developed bottom-level mine as shown in Fig. 2. The black circle refers to the stress changes at the VWSMs due to undermining (step 3). In step 2, the induced vertical stress is almost similar at the two sides of the instrumented pillars, P1 and P2, and any difference in the vertical stress can be attributed to differences in room width, pillar shape, and overburden depth. The VWSM in P2-pillar is closer to the floor resulting in a vertical stress slightly higher than that in P1-pillar. The extraction ratio for the top-level mine ranges from 80 to 85% based on the layout shown in Fig. 2, so the average pillar stress for a 119-m (390.3-ft) depth of cover based on the tributary area method would range from 15 to 20 MPa (2,175 to 2,900 psi). This stress is significantly less than the rock mass strength of limestone.

Although the overburden depth at the study site is relatively shallow, 119 m (390.3 ft), an 8 m (26.2 ft) of interburden thickness between the two mining levels is not enough to completely isolate the two levels. However, the stress transfer is relatively small. In step 3, the side of the upper-level pillar closer to the lower-level mined-out area experienced either stress relief or less stress concentration compared to the other side of the pillar, which is closer to the unmined/solid area. The reason for this behavior is that the side of the upper-level pillar that is closer to the lower-level mined-out area experienced less constraint and more displacement compared to the other side closer to the unmined area.

Based on instrumentation results, the stress change at VWSMs ranged from 0.40 to 0.70 MPa (58 to 101 psi), while the FLAC3D model predicted a stress change at the two stress

meters ranging from 1 to 2 MPa. Hence, the model matches relatively well the stress change at the stress meters (Fig. 3).

6 Influence of Pillar Offset on Stress Distributions in the Study Pillar

The FLAC3D numerical model shown in Fig. 1 was used to investigate the influence of pillar offsets on pillar stability in multiple-level mining conditions. As mentioned previously, the study pillar is located in the middle of a 9×9 array of pillars in the top-level mine. Designing a stable pillar in multiple-level mining conditions requires determining the locations and magnitude of stress concentrations, which depends to a great extent on the interburden thickness, pillar offset, extraction ratio, in situ stress conditions, and depth of cover. Figure 4 shows the variation of elastic vertical stress distributions at various pillar overlap percentages for 8-m (26.2-ft) interburden thickness. These stress distributions were taken along a cross-section at mid-pillar height and mid-pillar width of the study pillar. The pillar overlap percentages shown in Fig. 4 reflect pillar offset in the x direction only. The modeled pillars are located at 400 m (1,312 ft) depth of cover, and the horizontal/vertical stress ratio was 0.3. This depth is slightly larger than what is typically encountered in underground limestone mines. However, similar trends were found at other overburden depths. An extraction ratio of 0.75 was assumed in this study since it is the most common extraction ratio in underground stone mines [3].

The thick black “stepped” line (Development_top) shown in Fig. 4 represents the vertical stress distribution along the study pillar when the top-level mine was completely mined out, while the dotted red line (100%_overlap) represents the vertical stress distribution when both top and bottom-level mines were completely mined out and the pillars are stacked. When the pillars are stacked (100% pillar overlap), the induced vertical stress at the ribs of the study pillar slightly changed, due to the lower-level mine, while it noticeably increased at the pillar core.

Pillar offset generates asymmetric stress distribution such that stress concentration is higher on one side of the study pillar compared to the other side; these stress concentrations could be very high depending on the magnitude of the pillar offset and interburden thickness, which might lead to local instabilities and failures. Stress concentration occurred at both sides/edges of the study pillar when the pillar overlap percent was 100%, 8%, and 0%. While stress concentration occurred at one side of the study pillar, stress relief occurred at the other side according to all other pillar overlap percentages. The highest stress concentration occurred when the pillar overlap percent ranged from 67 to 33%, i.e., for 8-m interburden thickness, and the degree of interaction between the mining levels is highest when the pillar overlap percent ranges from 67 to 33%. Similar trends were found for high horizontal stress conditions (k -ratio = 3.0). The ratio of the induced maximum vertical stress at the pillar edge for 34% to a 100% overlap (stacked conditions) was about 1.15. This ratio is called the stress concentration factor. Table 3 summarizes the expected stress concentration factor from elastic material models at various interburden thickness when the depth of cover was 400 m (1,312 ft) and the k -ratio = 0.3.

To better understand the impact of pillar offset on pillar stability in multiple-level mining conditions, refer to Fig. 5, which shows the vertical stress distribution from FLAC3D models for 8-m (26.2-ft) interburden thickness at a pillar overlap percent of 100% and 0% when the k -ratio = 0.3 and the depth of cover = 400 m (1,312 ft). It is obvious that the vertical stress increases substantially at the overlap portions of the pillars for 50% pillar overlap and relieves elsewhere except the corners. Such high stresses could cause local pillar instabilities. To reduce the risk of the local pillar failures in multiple-level mining conditions, it is important to keep the pillar overlap percent close to 100%. The importance of stacking the pillars increases particularly if the interburden thickness is thin or the limestone material is weak.

The degree of interaction between mining levels increases with a reduction in the interburden thickness as shown in Figs. 6, 7, and Table 3. Figure 6 shows variation of the vertical stress distribution from elastic material models—at mid-pillar height—for 4 and 16-m (13.1 and 52.4-ft) interburden thicknesses and 400-m (1,312-ft) depth of cover. It is apparent that the interaction between the mining levels significantly reduced when the interburden thickness increased from 4 m (13.1 ft) to 16 m (52.4 ft), and the significance of pillar offset on pillar stability decreases with increasing the interburden thickness.

When the pillar overlap percent was 34% and the interburden thickness was 4 m (13.1 ft), the stress concentration factor was 1.5, while it was 1.02 when the interburden thickness was 16 m (52.4 ft). The stress concentration factor varies not only with the pillar overlap percent but also with depth. The higher the depth, the higher the stress concentration factor.

7 Local Pillar Instabilities Due to Multiple-Level Mining Conditions

Failure is a process by which a material changes from one state of behavior to another. More important types of material failures are yield and ultimate strength failure. In the following sections, nonlinear material models were used to examine the expected yield percentage and the ultimate strength of the study pillar at various pillar offsets, interburden thicknesses, and depths. The study pillar was examined when the top and bottom levels of the mine were fully developed.

Figure 8 shows the expected yielded pattern from two models subjected to the same conditions but different pillar offsets. Since pillar offsets resulted in asymmetric stress distributions where a portion of the study pillar is overstressed compared to the other portion, it is more logical/conservative to limit the analysis to the overstressed half of the study pillar rather than the whole entire study pillar if the pillars were offset in the x direction only. However, if pillars were offset in both the x and y directions, a quarter of the pillar will be overstressed compared to the other three quarters. Hence, the overstressed quarter of the study pillar will be investigated in such a case. The authors consider it more relevant to discuss here the potential for significant failures of rib from more localized stress concentrations due to pillar offset instead of the general yielding that may occur even in fully stacked geometries. To make this point clearer, suppose that the total number of failed (yielded) elements in the whole pillar is the same for both stacked and offset scenarios. For the offset scenario, most of the yielded elements are on one side of the pillar (see Fig. 8b),

while for the stacked scenario, an equal number of yielded elements occur on each side as shown in Fig. 8a. The thick black line shown in Fig. 8 divides the study pillar into two equal halves.

8 Influence of Interburden Thickness on Pillar Stability

In this section, the percentage yield is calculated for the overstressed half or quarter of the study pillar—not the entire study pillar—based on whether the pillars were offset in the x direction only or in the x and y directions. Figure 9 shows the variation of % yield at various degrees of pillar overlap and interburden thicknesses, when the depth of cover = 300 m (984 ft) and the k -ratio = 0.3, for (a) pillar offset in x direction only and (b) pillar offset in both x and y directions. The % yield is higher when pillars are offset in both the x and y directions, and hence, the pillar is at an elevated risk of failure in such a condition, particularly if the interburden thickness is thin and the depth of cover is high. The pillar offset has a substantial effect on % yield when the interburden thickness is thin. As the interburden thickness increases, the impact of pillar offset on pillar stability decreases. When the interburden thickness was 16 m or 32 m (52.4 ft or 104.9 ft), the pillar offset has less substantial effect on pillar % yield. It is obvious that the lowest degree of % yield in the study pillar (highest pillar stability) occurred when the pillars are stacked, while the highest degree of % yield (highest local instability) occurred between 10 and 70% pillar overlap. Similar trends were found for k -ratio = 3. However, the % yield is slightly less for the same conditions. It should be noted that again the interburden between mining levels was assumed elastic, preventing it from failing, and any interburden failure would impact pillar stability and might trigger pillar failure.

9 Influence of Depth on Pillar Stability in a Multiple-Level Mining Condition

To get a complete picture of the impact of pillar offset on pillar stability in multiple-level mining conditions, it is important to consider pillars at various overburden depths. Figure 10 shows the variation of % yield with pillar overlap percentage at various depths when the interburden thickness was 8 m (26.2 ft) for (a) pillar offset in the x direction only and (b) pillar offset in both the x and y directions. For 400 m (1,312 ft) depth of cover, significant % yield occurred even at 100% pillar overlap. This high % yield occurred during the development stage of the upper-level mine—the lower-level mine was not developed yet—because the induced stresses, corresponding to a 400 m (1,312 ft) depth of cover and an extraction ratio of 0.75, is high compared to the assumed rock mass strength.

The impact of pillar offset on pillar stability varies with depth. For shallow mines of 200 m (656 ft) or less, the numerical modeling results indicate that pillar offset is not an issue and its impact is not substantial on local pillar stability. Field observations at top-level pillars of Mine A—used to validate the FLAC3D model earlier—match well with the model results. However, field observations at bottom-level pillars at Mine A did show some effect of the pillar offset where the rib spalled off about 1 ft. The reason that these bottom-level pillars were affected more by pillar offset was because they are highly fractured compared to the top-level pillars.

The significance of pillar offset increases substantially for 300 m (984 ft) depth of cover, and it slightly reduces for 400 m (1,312 ft) depth of cover. Keep in mind that the expected % yield from FLAC3D models is highly dependent on the rock mass strength; if the rock mass strength is higher as assumed in this study, the expected % yield would decrease and vice versa.

10 Influence of the k -Ratio on Pillar Stability in a Multiple-Level Mining Condition

Unlike the roof, the strength and stability of stone pillars increase with increasing the k -ratio. The lateral confining stress generated from a higher k -ratio has the effect of strengthening the pillar. A smaller k -ratio may result in a very low compressive minimum principal stress or a tensile minimum principal stress that would increase the risk of failure. Figure 11 shows the influence of the k -ratio on pillar stability at various pillar offsets in the x direction for a 300-m (984-ft) depth of cover and interburden thickness of 4 and 8 m (13.1 and 26.2 ft). The blue lines represent the k -ratio of 3, while the black lines represent the k -ratio of 0.3. As shown in Fig. 11, the significance of pillar offset on pillar stability varies with the k -ratio and the interburden thickness. The significance of pillar offset on pillar stability is substantial for 8-m (26.2-ft) interburden thickness when the k -ratio was 0.3, although it was not substantial when the k -ratio was 3.0. On the other hand, the pillar offset was substantial for 4-m (13.1-ft) interburden thickness no matter what the k -ratio is.

11 Influence of Pillar Overlap Percentage and Interburden Thickness on Pillar Strength

Pillar peak strength is a state at which the pillar changes from gradually increasing load-bearing capacity to a constant or a gradually decreasing load-bearing capacity. In FLAC3D, in order to establish the peak strength of the study pillar, a vertical velocity at the top of the model is fixed at a constant value of -0.5×10^{-6} m/step to fail the study pillar. The vertical stress and strain for all elements composing the study pillar was averaged via a *FISH* function at each step. The authors did not find a significant difference between averaging the vertical stress for all elements composing the study pillar and averaging vertical stress at mid-pillar height. Figure 12 shows the influence of pillar offset on pillar strength at various interburden thicknesses when the k -ratio is 0.3. Similar trends were found when the k -ratio = 3.0. However, the pillar strength was slightly higher than that shown in Fig. 10. As mentioned previously, interburden stability was not considered in this study, i.e., the interburden is elastic and never fails. Interburden failure might trigger pillar failure or place the pillar at more risk of failure.

For 4-m (13.1-ft) interburden thickness, the pillar strength decreases with increasing the pillar overlap percentage. The pillar lost about 33% of its strength when the pillar overlap percent changed from 100 to 0%. The reason for such high reduction in pillar strength is that the degree of constraint that the floor provides the pillar is decreasing with increasing the pillar overlap percentage since part of the pillar is underlain by a void, i.e., the floor portion under the study pillar is not fully fixed, which is why pillar strength was substantially

reduced. For 8-m (26.2-ft) interburden thickness, the average strength of the pillar was slightly affected when the pillar overlap percent changed from 100 to 0%. While for 16 and 32 m (52.4 and 104.9 ft), the pillar strength was minimally affected by the pillar offset.

12 Conclusion

In this study, FLAC3D numerical models were used to understand the impact of numerous factors on limestone pillar stability in multiple-level mining conditions. The models have been validated with field instrumentation results at a multiple-level underground limestone mine. It has been assumed in the models that both the interburden and the roof spans are stable. The results and conclusions drawn from this work are not applicable to structurally controlled rock masses where a single plane of weakness was oriented at an unfavorable orientation. However, it is applicable to fractured rock masses where all structural features are equally likely.

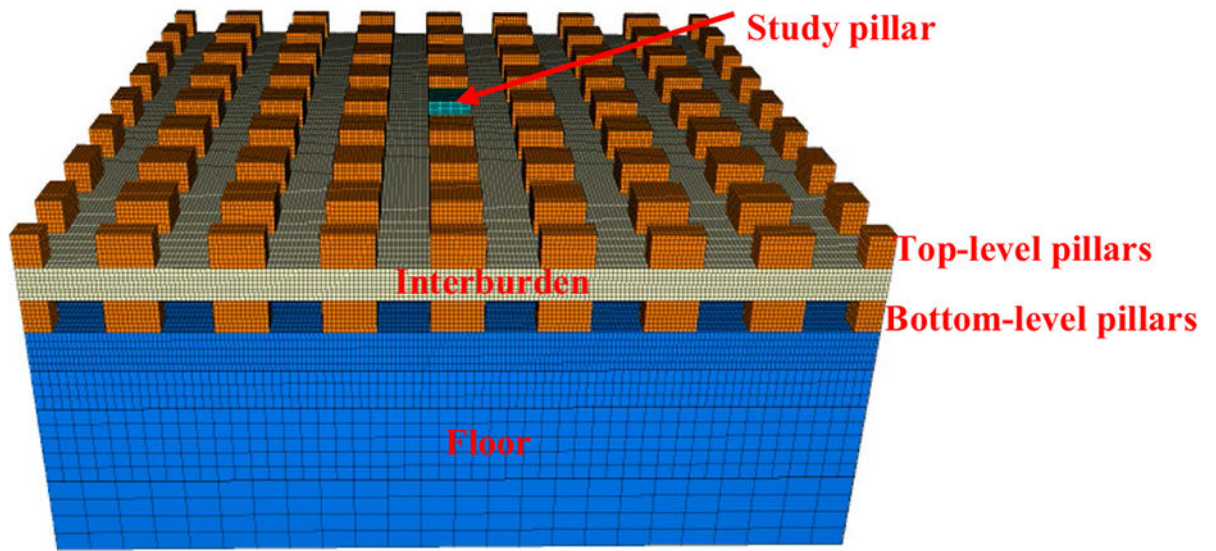
The authors found that whether an adverse pillar instability occurs or not depends on numerous factors, such as overburden depth, interburden thickness, pillar overlap percent, and in situ stress conditions. A combination of these factors may result in various degrees of multiple-level mining interaction, with some being significantly unfavorable that will put the limestone pillar at risk of local instability. The highest degree of pillar stability occurred when the pillars are fully stacked, while the highest degree of local instability occurred when the pillar offset ranged from 10 to 70%. When the depth of cover was less than 200 m (656 ft), pillar offset (pillar overlap percent between mining levels) does not appear to be an issue when the interburden thickness was 8 m (~ 26 ft) given that the roof span is 12 m (~ 40 ft). Within the range of the study parameters, the degree of interaction between the mining levels was minimum when the interburden thickness was greater than 16 m (26.2 ft) which is about 1.33 of the roof span. However, the underlying assumption is that the interburden is elastic (never fails) and an interburden failure might trigger pillar failure. The high horizontal stresses provide the pillar with more strength and reduces the impact of pillar offsets on pillar stability.

The effect of the study parameters is intended to provide insight into the ground control interactions between multiple mining levels in underground stone mines. There is future work to be done regarding different material properties and pillar geometries, but the relative effect of the parameters tested in this study should provide a starting point for understanding local pillar stability due to multiple-level mining conditions in underground stone mines, which ultimately leads to more stable designs that increase the safety of mine workers.

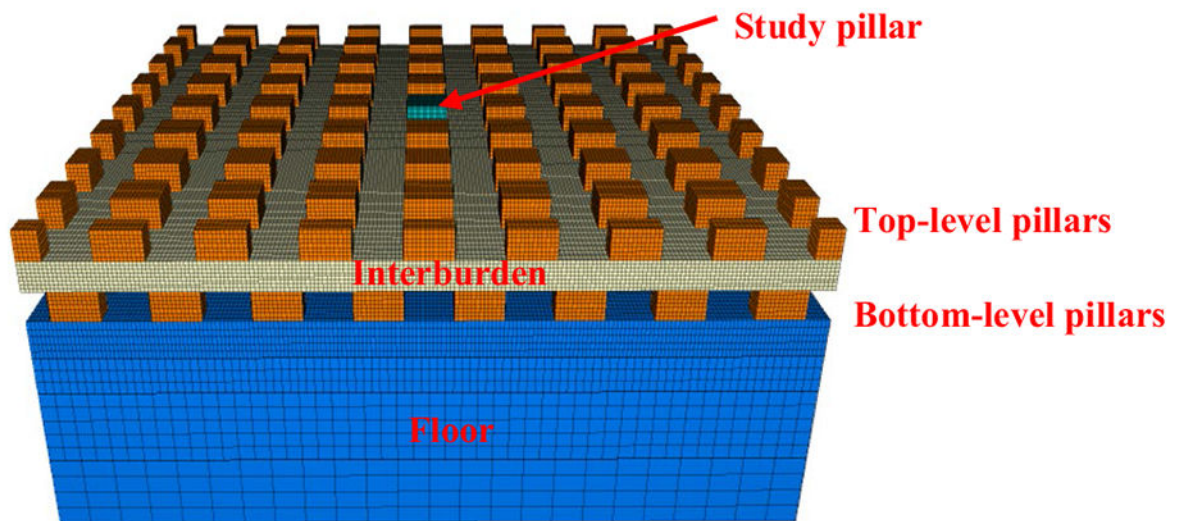
References

1. American Society for Testing Materials (ASTM), "Standard test method for compressive strength and elastic moduli of intact rock core specimens under varying states of stress and temperatures," ASTM D 7012-04 Methods A, C and D, ASTM, West Conshohocken, PA, 1429–1436
2. Esterhuizen GS, Murphy MM (2018) Mining Product: S-Pillar - Software for Stone Mine Pillar Design Version 1.2. Pittsburgh, PA: U.S. Department of Health and Human Services, Public Health Service, Centers for Disease Control and Prevention, National Institute for Occupational Safety and Health, <https://www.cdc.gov/niosh/mining/works/cover-sheet1817.html>

3. Esterhuizen GS, Dolinar DR, Ellenberger JL, Prosser LJ (2011) Pillar and roof span design guidelines for underground stone mines. Department of Health and Human Services, Public Health Service, Centers for Disease Control and Prevention, National Institute for Occupational Safety and Health, DHHS (NIOSH) Publication No. 2011–171, IC 9526, <https://www.cdc.gov/niosh/mining/UserFiles/works/pdfs/2011-171.pdf>
4. Esterhuizen GS, Ellenberger JL (2007) Effects of weak bands on pillar stability in stone mines: field observations and numerical model assessment. In: Proceedings of the 26th International Conference on Ground Control in Mining, Morgantown, WV: West Virginia University, 320–326
5. Haycocks C, Zhou Y (1990) Multiple-seam mining: a state-of-the-art review. In: Proceedings of the Ninth International Conference on Ground Control in Mining, Morgantown, WV: West Virginia University, 1990, 1–11
6. Hoek E, Brown ET (2018) The Hoek-Brown failure criterion and GSI – 2018 edition. *J Rock Mech Geotech Eng.* 10.1016/j.jrmge.2018.08.00
7. Hoek E, Diederichs MS (2006) Empirical estimation of rock mass modulus. *Int J Rock Mech Min Sci* 43(2):203–2015
8. Hsiung SM, Peng SS (1987) Design guidelines for multiple-seam mining, Part II. *Coal Mine Process States*, vol. 24, no. 10
9. Iannacchione T (1999) Analysis of pillar design practices and techniques for U.S. limestone mines. *Trans Inst Min Metall (sect. A: Min. Industry)*, September–December 108: A152–A160
10. Itasca Consulting Group (2018) Fast Lagrangian analysis of continua in 3dimensions. Itasca Consulting Group: Minneapolis, MN, USA
11. Lunder PJ, Pakalnis RC (1997) Determination of the strength of hard-rock mine pillars. *Bull Can Inst Min Metall* 90(1013):51–55
12. Mark C, Tuchman RJ (2007) Proceedings: new technology for ground control in multiple-seam mining. Department of Health and Human Services, Public Health Service, Centers for Disease Control and Prevention, National Institute for Occupational Safety and Health, DHHS (NIOSH) Publication No. 2007–110, Information Circular 9495.
13. McNeel R, others (2010) Rhinoceros 3D, Version 6.0. Robert McNeel & Associates, Seattle, WA
14. Murphy M, Esterhuizen GS, Slaker B (2020) Addressing stone mine pillar design with the NIOSH S-Pillar software. SME Annual Meeting, Feb. 24 - 27, Phoenix, AZ
15. Newman C, Newman D, Dupuy R (2020) Development of a multiple level underground limestone mine from geology through mine planning. *Int J Min Sci Technol* 30(1):63–67. 10.1016/j.ijmst.2019.12.007
16. Newman D (2017) Roof control pillar stability and ground control issues in underground stone mines. *Min Eng* 69(8):53–58. 10.19150/me.7685
17. Newman DA, DeCinque J, Dafferner A (2001) The integration of geology and engineering in ground control and mine planning for a multi-level underground limestone quarry. In: Proceedings of the 20th International Conference on Ground Control in Mining, Morgantown, WV: West Virginia University, 7–9 August 2012
18. Rashed G, Slaker BA (2020) A study of the interburden stability in multilevel limestone mines using FLAC3D models. Paper presented at the 54th U.S. Rock Mechanics/Geomechanics Symposium, physical event cancelled. vol. 64, p. 75.
19. Slaker B, Murphy M, Rashed G (2020) Monitoring of multiple-level stress interaction at two underground limestone mines. *Min, Metall Explor.* 10.1007/s42461-020-00345-z



a)



b)

Fig. 1. Schematic for **a** stacked (columnized) pillars and **b** zero % overlap between top and bottom level pillars. The study pillar is in the middle of the pillar array

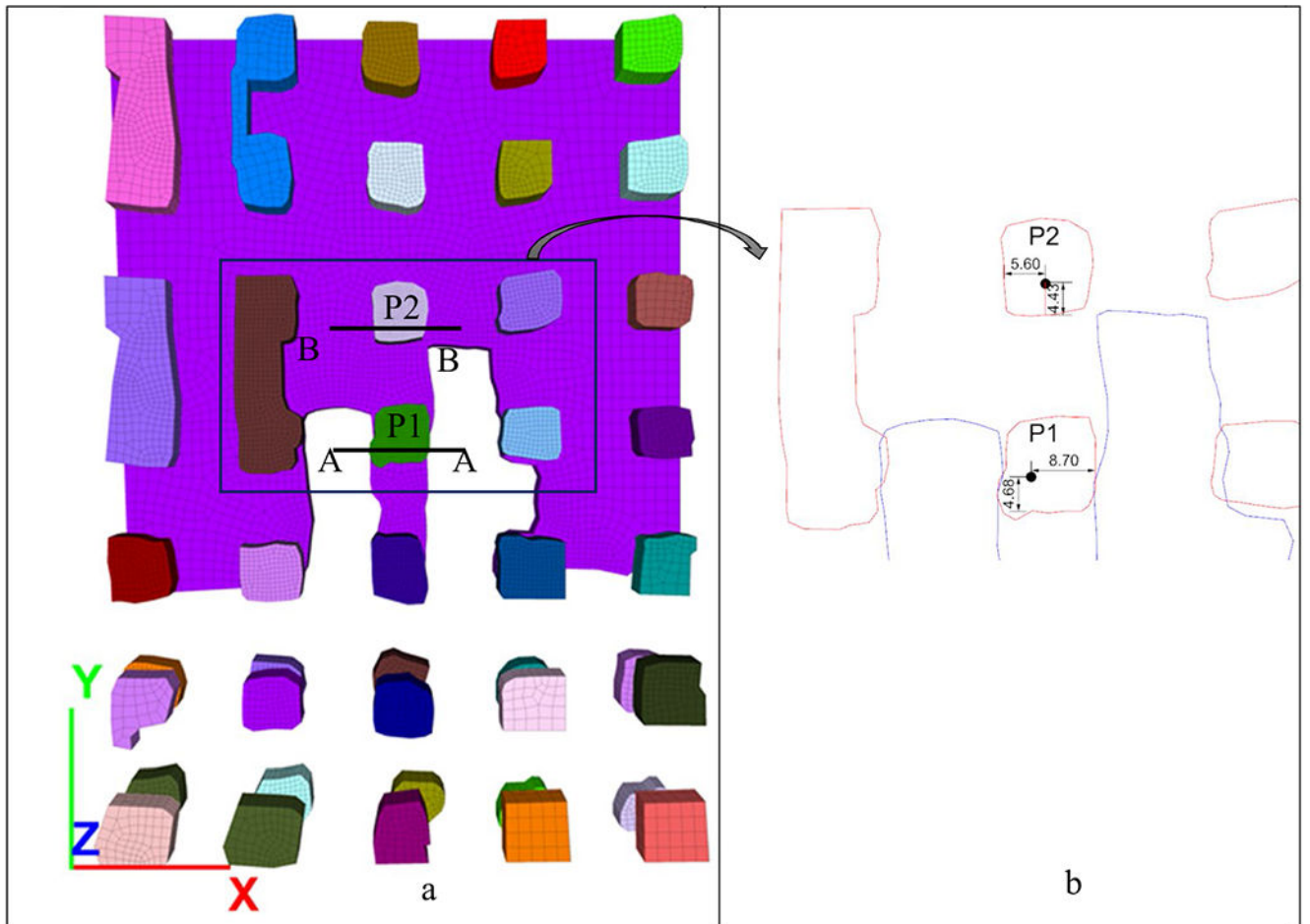


Fig. 2.
a Top and bottom levels mine overlain on each other, **b** P1 and P2 are instrumented with VWSM, top mine is outlined in red, and bottom mine is in blue. A-A and B-B are two cross-sections along the VWSMs

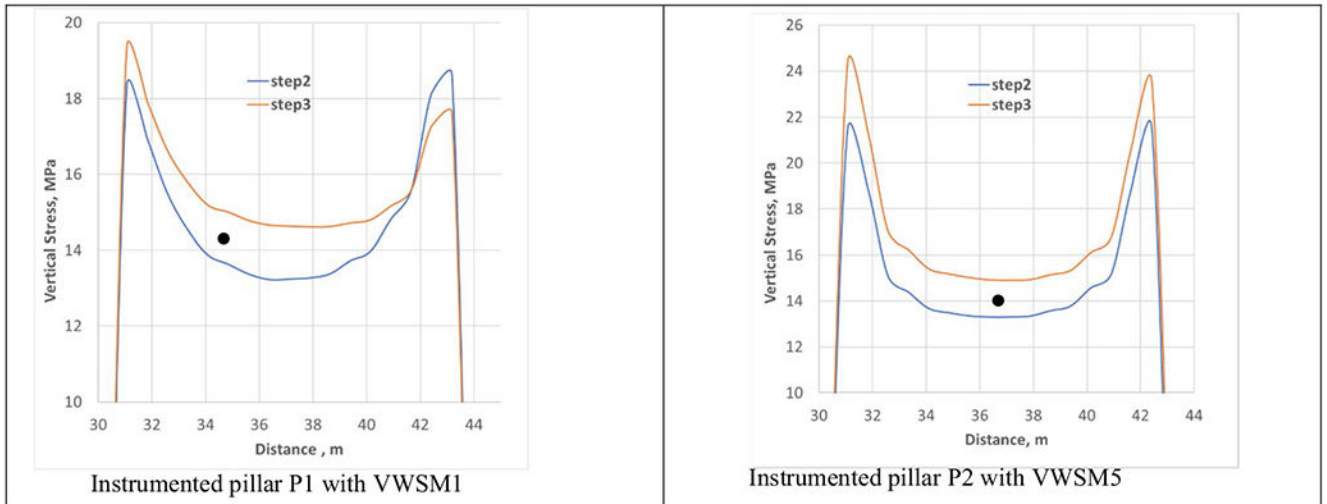


Fig. 3. Vertical stress distribution across instrumented pillars P1 and P2 for step 2 and step 3. The black circle represents the measured vertical stress at step 3

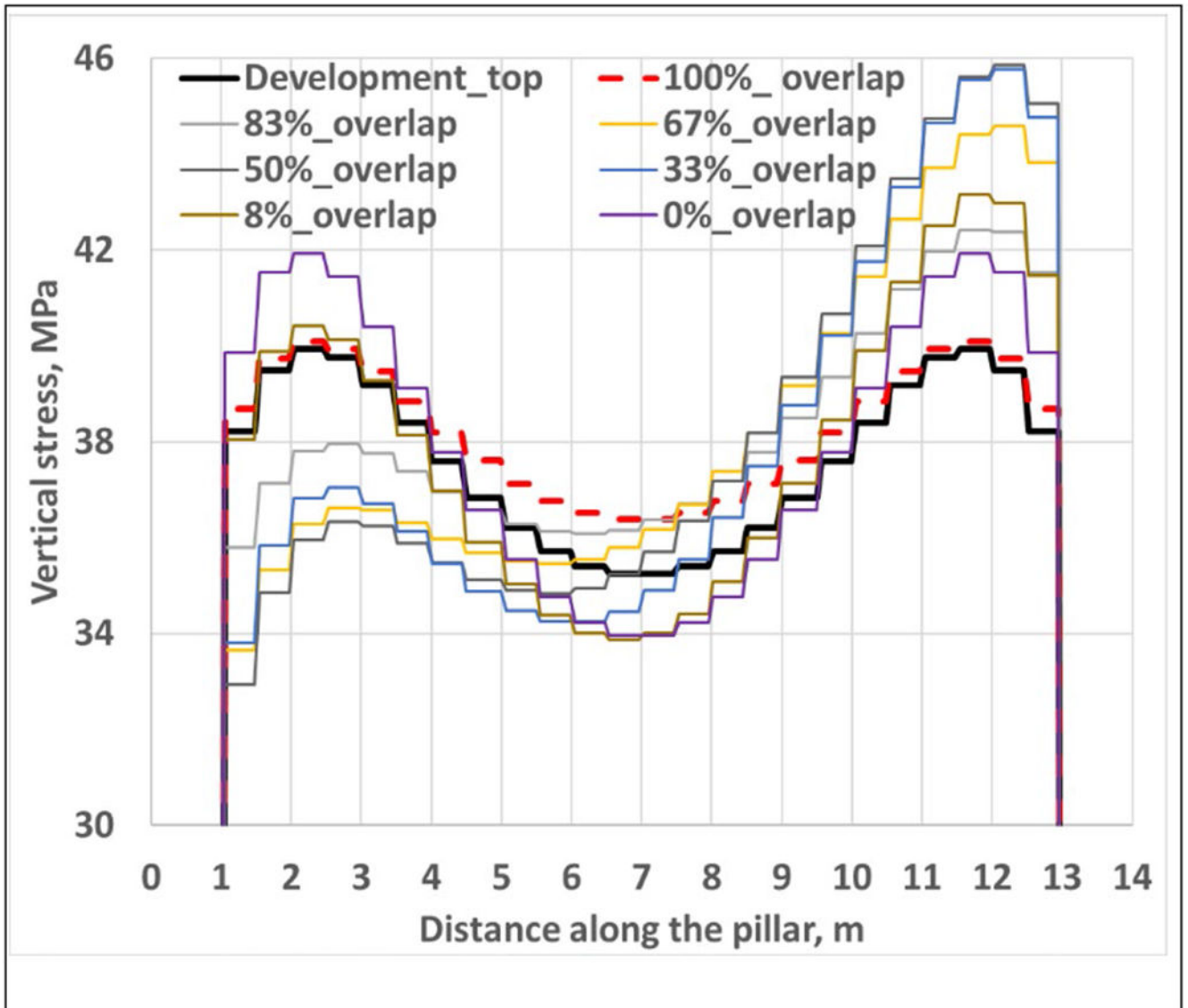


Fig. 4. Variation of vertical stress distributions with pillar overlap percent for 8-m interburden thickness, k -ratio = 0.3, and the depth of cover = 400 m. The pillar overlap percentage is due to pillar offset in the x direction only

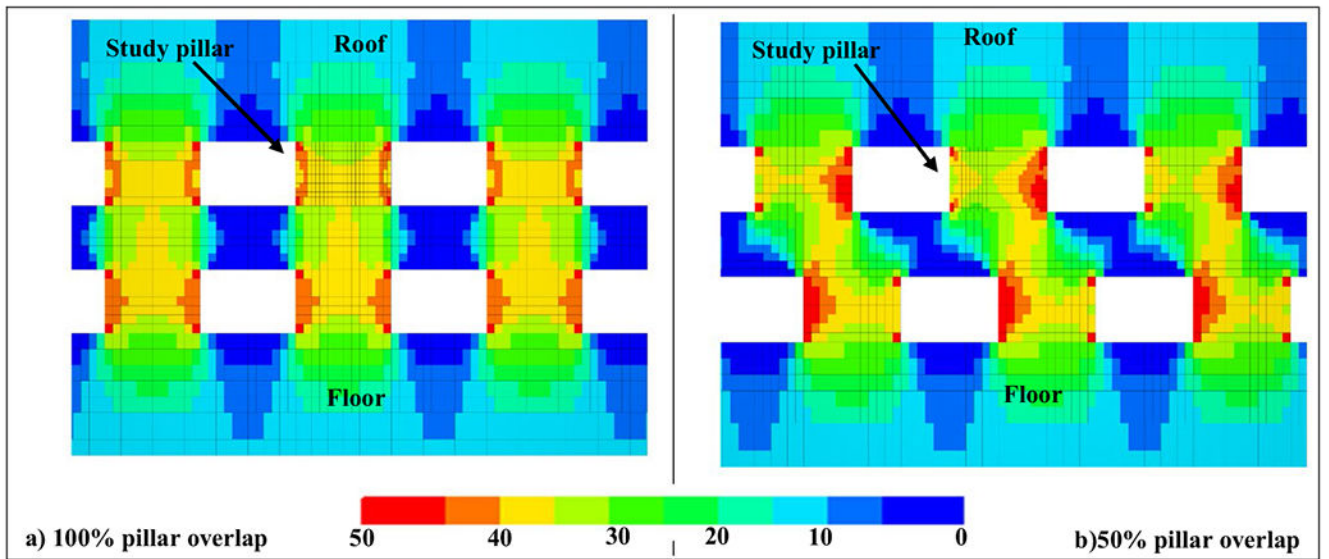


Fig. 5. Vertical stress distribution at 400-m depth of cover and k -ratio = 0.3 for **a** 100% pillar overlap and **b** 50% pillar overlap. Stress values are in MPa. Pillar overlap percent is due to pillar offset in the x direction only

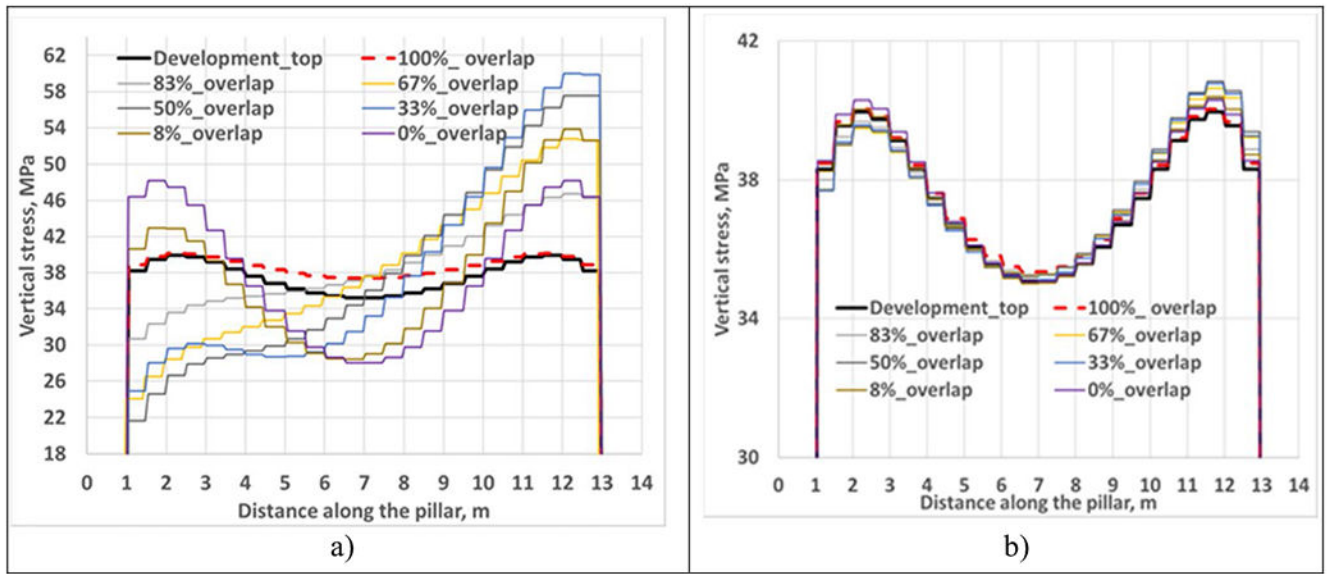


Fig. 6. Variation of vertical stress distributions with a pillar overlap percentage for **a** 4-m (13.1-ft), **b** 16-m (52.4-ft) interburden thicknesses, k -ratio = 0.3, and the depth of cover = 400 m (1,312 ft)

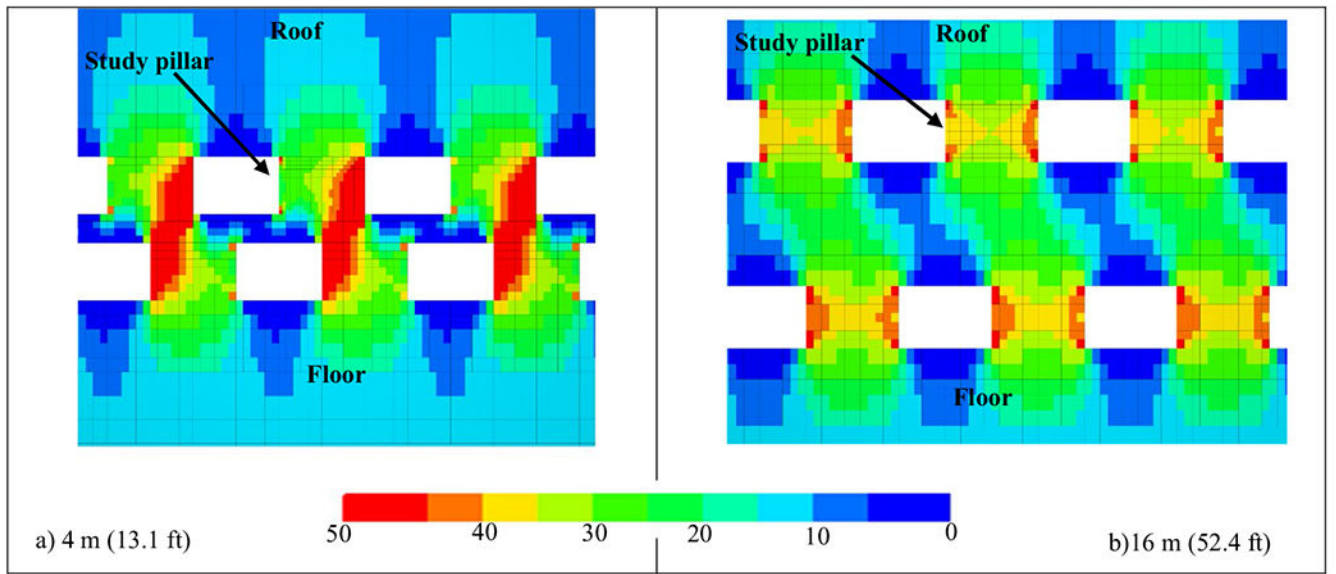


Fig. 7. Vertical stress distribution at 400 m (1,312 ft) depth of cover and k -ratio = 0.3 for **a** 50% pillar overlap and **b** 50% pillar overlap. Stress values are in MPa. The pillar overlap percentage is due to pillar offset in the x direction

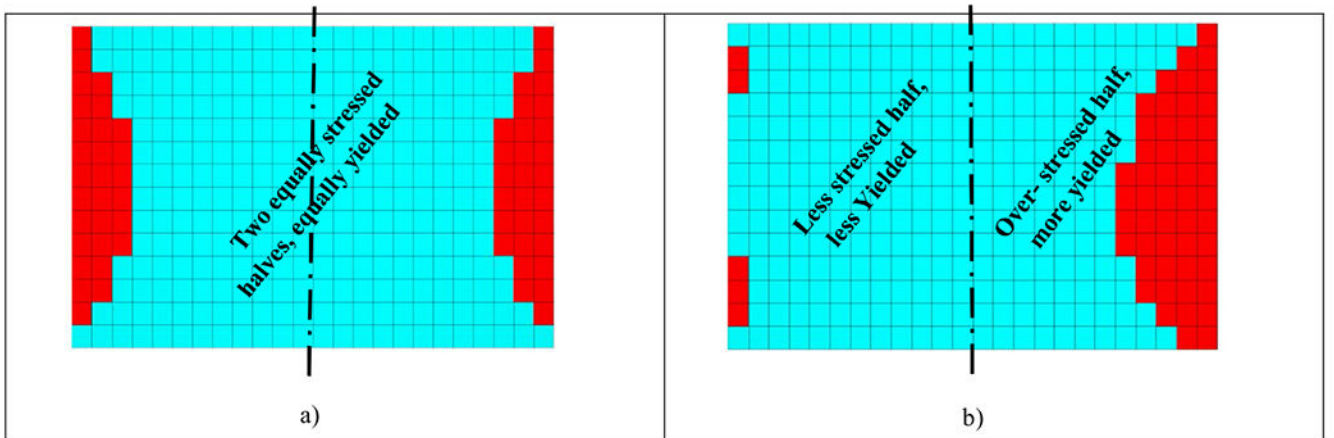


Fig. 8. Yielded pattern for two models at the same conditions but different pillar offsets. Red elements are yielded, while blue elements are elastic

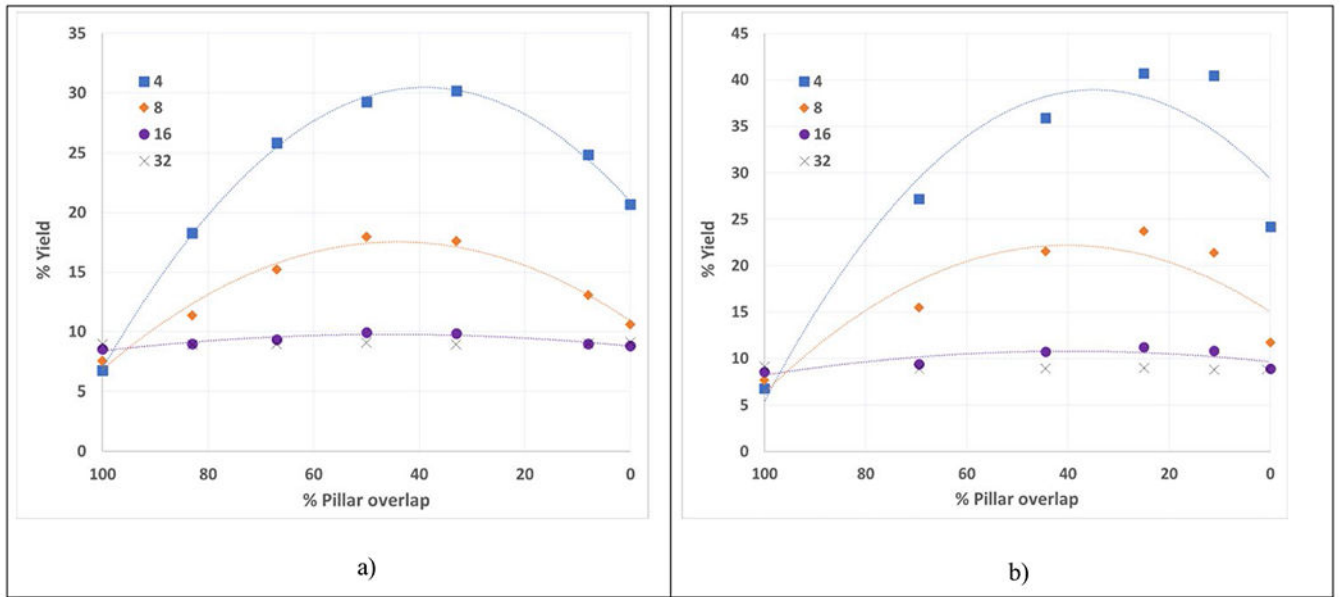


Fig. 9. Influence of interburden thickness on % yield at various pillar offsets for **a** pillar offset in the *x* direction and **b** pillar offset in both the *x* and *y* directions; the depth of cover = 300 m (984 ft) and the *k*-ratio = 0.3

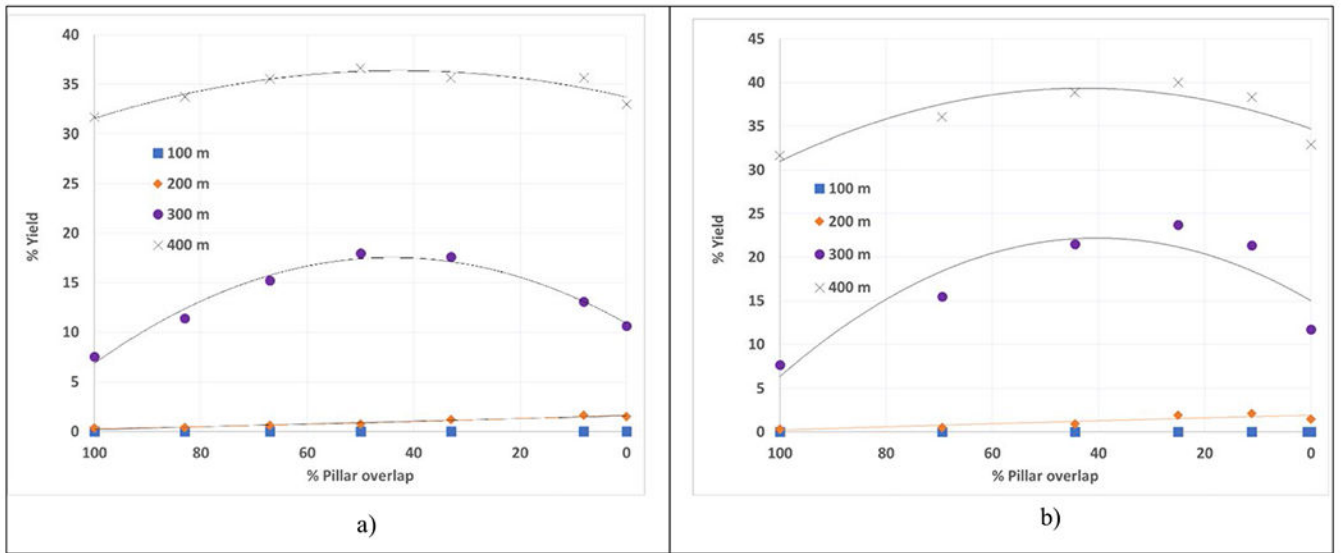


Fig. 10. Influence of depth on % yield at various pillar offsets for **a** pillar offset in x direction only and **b** pillar offset in both x and y directions. The interburden thickness = 8 m (25.2 ft)

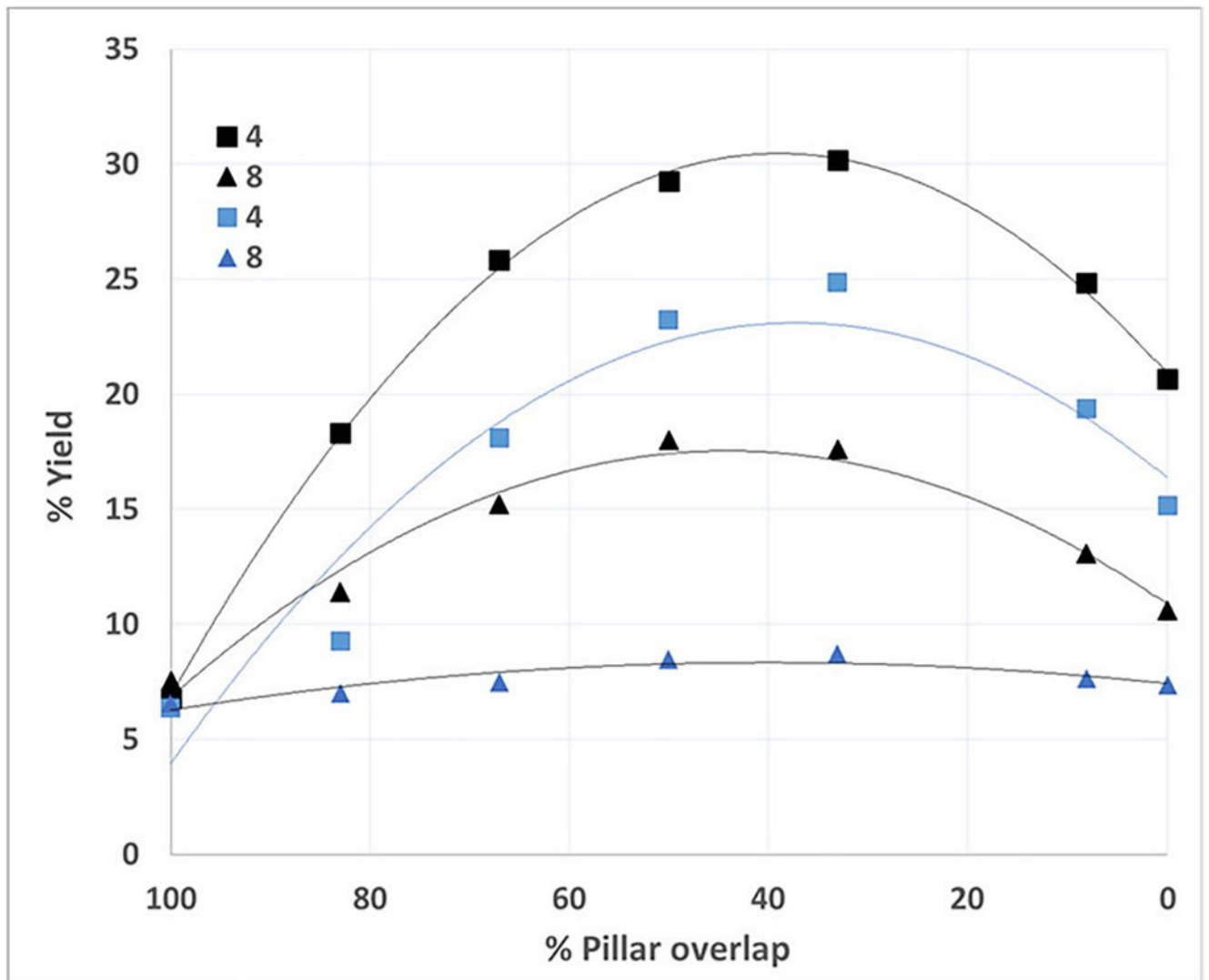


Fig. 11. Influence of k -ratios on % yield at various pillar offsets for 4- and 8-m (13.1- and 26.2-ft) interburden thicknesses at a depth of cover = 300 m (984 ft). Black lines are for k -ratio = 0.3, and blue lines are for k -ratio = 3.0

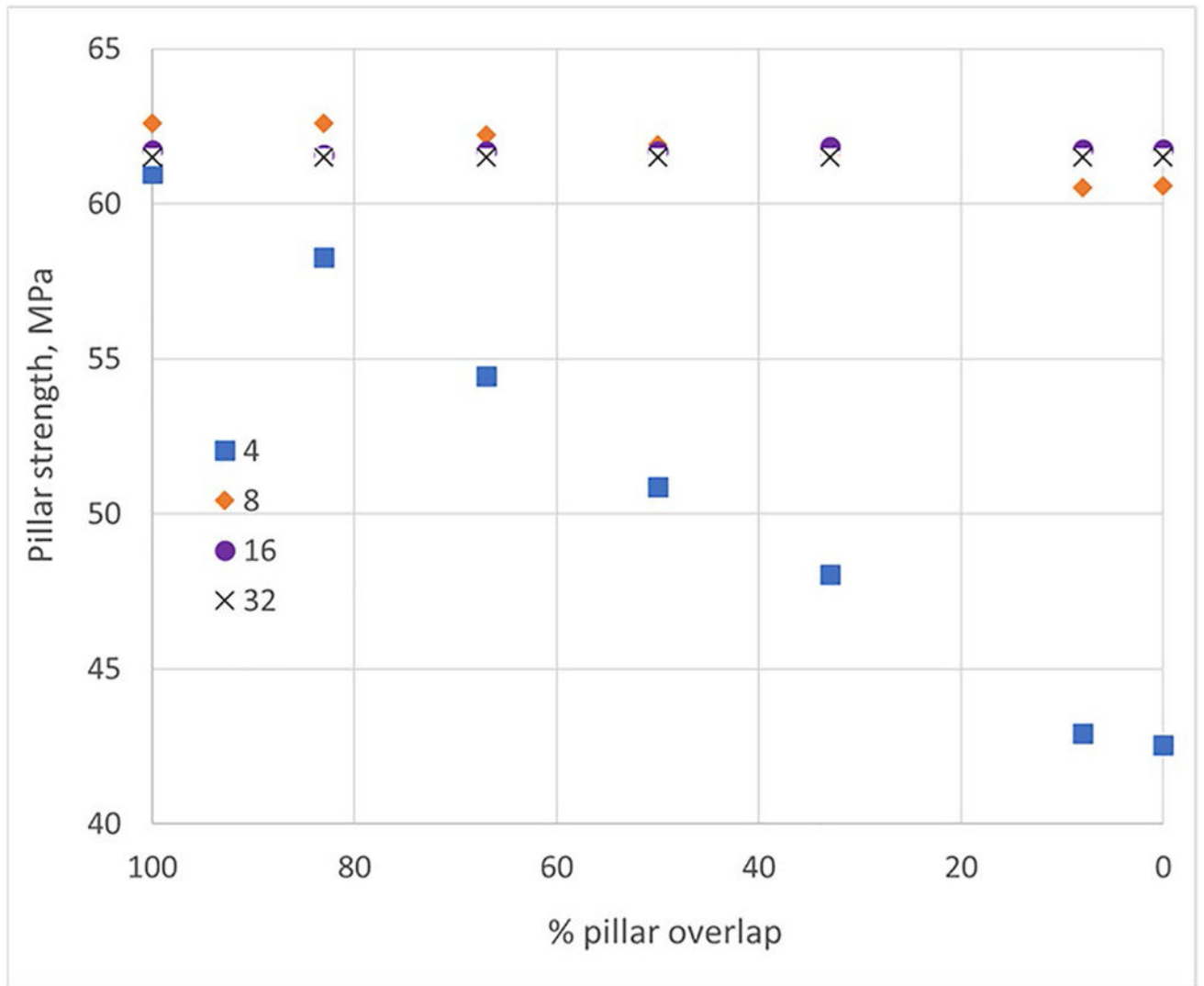


Fig. 12.
Pillar strength at various interburden thicknesses and pillar offsets for k -ratio of 0.3

Table 1

Summary of the study parameters used in the FLAC3D models

Parameter	Parameter values evaluated
Depth, m (ft)	100 (328), 200 (656), 300 (984), and 400 (1,312)
Interburden thickness, m (ft)	4 (13.1), 8 (26.2), 16 (52.4), and 32 (104.9)
Pillar overlap in x direction, %	100, 83, 67, 50, 33, 8, and 0
Pillar overlap in x- and y directions, %	100, 69, 44, 25, 11, and 0
k-ratio	0.3 and 3.0
Pillar width-to-height ratio	1.5
Roof span, m (ft)	12 (~40)
Material model	Linear and nonlinear

Table 2

Summary of laboratory test results for the limestone specimens used in this study

Parameter	Value
Unconfined compressive strength (UCS), MPa (psi)	100 (14,500)
Poisson's ratio (ν)	0.25
Intact Young's modulus (E_i), GPa (psi)	50 (7.25 E6)
Hoek-Brown m_i parameter	9.98
Hoek-Brown s parameter	1.0

Author Manuscript

Author Manuscript

Author Manuscript

Author Manuscript

Stress concentration factor at various interburden thicknesses for 400 m (1,312 ft) depth of cover and k -ratio = 0.3

Table 3

Interburden thickness, m (ft)	Pillar overlap percent in x direction						
	100%	83%	67%	50%	34%	8%	0%
4 (13.1)	1	1.16	1.31	1.43	1.50	1.34	1.20
8 (26.2)	1	1.06	1.11	1.15	1.15	1.07	1.05
16 (52.4)	1	1.01	1.02	1.02	1.02	1.01	1.01
32 (104.9)	1	1	1	1	1	1	1